



Deliverable Number: D 18.09

Deliverable Title: [Extending the technique towards ToF-imaging](#)

Delivery date: 48

Leading beneficiary: PSI, HZB (5,6)

Dissemination level: Public

Status: completed

Authors: N. Kardjilov

Project number: 283883

Project acronym: NMI3-II

Project title: Integrated Infrastructure Initiative for Neutron Scattering and Muon Spectroscopy

Starting date: 1st of February 2012

Duration: 48 months

Call identifier: FP7-Infrastructures-2010

Funding scheme: Combination of CP & CSA – Integrating Activities

Extending the technique towards ToF-imaging

A recent study at the neutron imaging instrument at HZB CONRAD-2 showcased the use of the Bragg-edge mapping technique by separating and quantifying different crystallographic phases in metastable stainless steel (ASTM standard 304L) that exhibits the TRIP effect (Woracek *et al.*, 2014). Several samples were subjected to certain plastic tensile and torsional strains, inducing a martensitic phase transformation, where austenite (having a face-centered cubic structure, fcc) transforms to martensite (consisting of body-centered cubic, bcc, and hexagonal closest packed, hcp, structures). Radiographs of samples with varying amounts of Austenite and Martensite were recorded at several wavelengths. Figure 1b shows the transmission spectra obtained for three different samples (regions) with a thickness of 8 mm, where the wavelength increment between each radiograph was 0.02 Å and the integration time for each image was 2 minutes. As a reference, Figure 7c shows an example for transmission spectra, obtained for the same samples in *time-of-flight mode* at a spallation source with an energy resolution of 0.4%, where a shoulder-like double edge is visible for the sample with 60% Austenite. However, phase discrimination is also possible with the reduced resolution of the monochromator, even though only one Bragg edge is visible around the “Bragg cut off” for mixed phases. The position (and rise) of this observed edge is directly influenced by the phase fraction. At CONRAD-2, tomographic scans were performed by recording 180 projections over a 360° range below (4.1 Å) and above (4.3 Å) the Bragg edge corresponding to the fcc(111) lattice planes of the austenitic phase. The exposure times were 2 minutes per projection, resulting in total measurement time of twelve hours for both wavelengths. The filtered back-projection algorithm for parallel beam reconstruction was used to reconstruct the tomographic data sets.

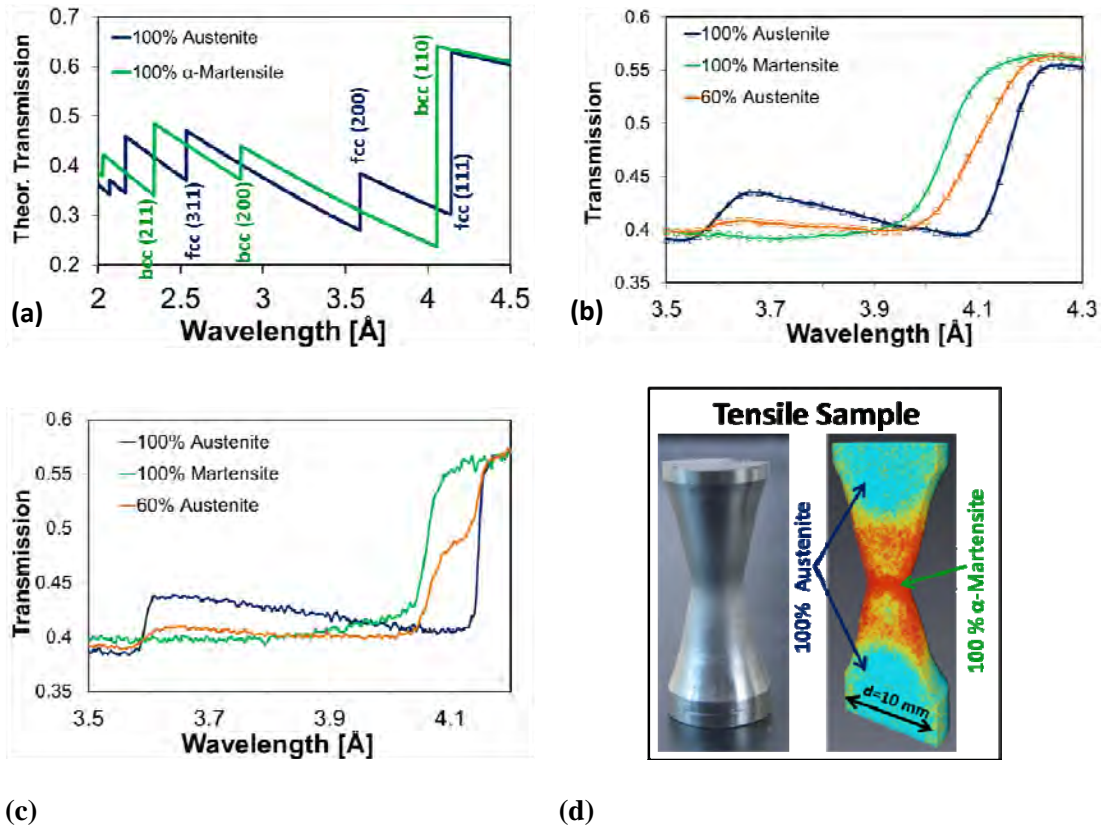


Figure 1: Example of energy-selective imaging. (a) Theoretical transmission values for Austenite and α -Martensite. (b) Experimentally measured transmission spectra at CONRAD-2 for iron samples of varying phase compositions. (c) A comparison of the same samples measured in *time of flight mode* at a spallation source with better wavelength resolution. (d) 3D reconstructed phase fractions, obtained at CONRAD-2, inside a plastically deformed tensile sample, where large plastic deformation leads to the formation of martensite.

At 4.1 \AA , the attenuation coefficient for regions with larger martensitic phase content is lower than for regions with more austenitic phase content, due to the differing Bragg edge positions. By normalizing the reconstructed data taken at 4.1 \AA by the data taken at 4.3 \AA , a ratio of the Bragg edge height is obtained that can be used for quantification of the phase fractions. Neutron diffraction was used at selected locations inside the samples, while EBSD was used on the surface of cut cross sections to verify the neutron imaging based results. All results show very good agreement (Woracek *et al.*, 2015).

Diffraction contrast imaging at the Bragg edges with monoenergetic neutrons can therefore be used as a complementary visualization and quantification tool to study phase transition effects in steels and other metals. It allows for non-destructive bulk investigations, can reveal inhomogeneities that may remain undetected if only diffraction is used, while other features visible in the tomography data (such as cracks, porosities, etc) can be visualized simultaneously.

References

- Woracek, R., Penumadu, D., Kardjilov, N., Hilger, A., Boin, M., Banhart, J. & Manke, I. (2014).
Advanced Materials **26**, 4069-4073.
- Woracek, R., Penumadu, D., Kardjilov, N., Hilger, A., Boin, M., Banhart, J. & Manke, I. (2015).
Physics Procedia **69**, 227-236.